SnO_2 nanoparticles in silica: Nanosized tools for femtosecond-laser machining of refractive index patterns

A. Paleari,[a] E. Franchina, N. Chiodini, and A. Lauria
CNISM and Dipartimento di Scienza dei Materiali, Università di Milano-Bicocca, via Cozzi 53, I-20125 Milano, Italy

E. Bricchi and P. G. Kazansky
Optoelectronics Research Centre, University of Southampton, Southampton SO17 1BJ, United Kingdom

(Received 22 July 2005; accepted 11 March 2006; published online 31 March 2006)

We show that SnO_2 nanoclusters in silica interact with ultrashort infrared laser pulses focused inside the material generating a hydrostatic compression and photoelastic response of the surrounding glass. This effect, together with the laser-induced nanocluster amorphization, gives rise to positive or negative refractive-index changes, up to 10^{-2}, depending on the beam-power density. This result points out a wide tuning of the refractive index patterns obtainable in silica-based optical technology. © *2006 American Institute of Physics*. [DOI: 10.1063/1.2192579]

In the last decade, the ability of lasers to induce a modification of the optical properties in silica-based materials became matter of extensive investigation.[1–7] Indeed, a photoinduced modification of the refractive index can be utilized to create waveguides, gratings, and other optical patterns for integrated photonic devices in a one-step technique. In this framework, the photorefractive response of a nanostructured composite may be drastically innovative. In fact, different responses of coexisting phases to the laser radiation are expected to give rise to concomitant and possibly interacting processes to achieve a wide tuning of refractive index. Wide-band-gap nanophases in silica are promising systems in this regard, since their optical properties would allow the laser machining inside the bulk. In such a system, i.e., a silica composite containing SnO_2 nanocrystals,[8] we recently found a negative photosensitivity to unfocused ultraviolet and visible lasers.[9,10] In this work we demonstrate the feasibility of writing a buried pattern of refractive index n with either negative or positive Δn by varying the power density of a focused beam of an infrared femtosecond laser.

We have analyzed femtosecond-laser writing processes in nanostructured optical grade SiO_2:SnO_2 glass ceramics (84:16 molar ratio) synthesized from a sol-gel route,[8] together with a reference silica sample. An amplified mode-locked Ti:sapphire laser operating at 800 nm (200 fs pulse duration) was used to irradiate the samples. Squares of $100 \times 100\ \mu m^2$ were written at about 250 μm from the surface, at different pulse energy values, by writing adjacent lines spaced 1 μm apart at a speed of 80 μm/s with the beam polarization orthogonal to the lines. Two focusing configurations were used with high and low numerical apertures (NAs) (0.55 and 0.21, respectively). Images of the written patterns, in unpolarized light and through two crossed polarizers, are reported in Fig. 1.

The laser-induced modification Δn with respect to the unprocessed bulk was measured from the change of optical path experienced by a polarized probe beam at 633 nm on traversing the sample. Possible laser-induced birefringence[7] was investigated analyzing the phase $\Delta\Phi_{xy}$ and $\Delta\Phi_{xx}$ for the orthogonal and parallel directions with respect to the writing polarization. Structural modifications along the z axis of laser propagation were analyzed by confocal micro-Raman spectroscopy. Changes of nanometric structure were analyzed by transmission electron microscopy (TEM).

Figure 2 summarizes the interferometry results. The negative $\Delta\Phi$ in glass ceramic after low-NA irradiation is

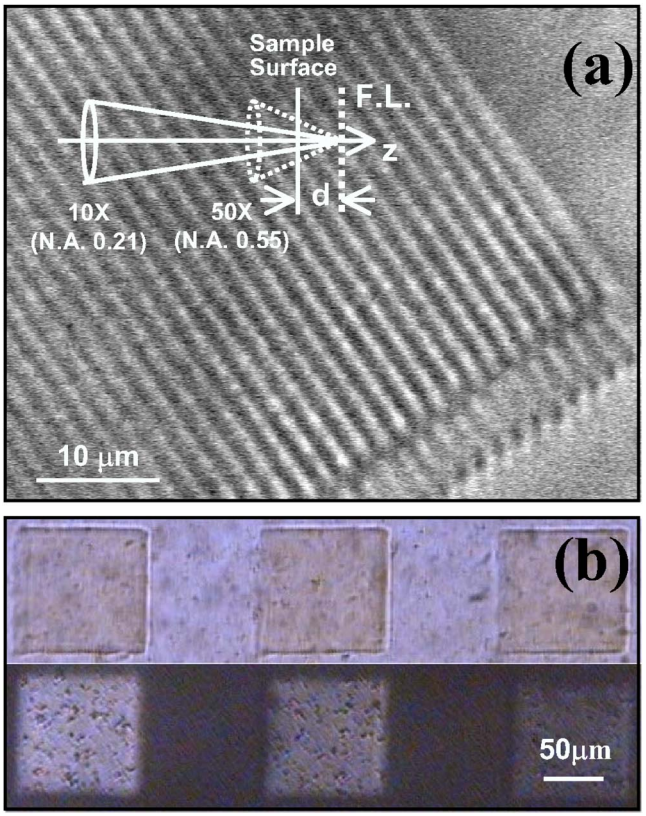

FIG. 1. (Color online) (a) Optical microscopy image of a refractive index pattern photowritten in SnO_2:SiO_2 glass ceramic. The white-drawn picture is a schema of the high-NA (dotted line) and low-NA (straight line) configurations used for focusing the laser beam at the focal layer (FL). (b) Direct written patterns processed at different pulse energies: 1.5, 1.25, and 1 μJ from left to right, with unpolarized light (top) and with the sample between crossed polarizers (bottom).

[a]Electronic mail: alberto.paleari@mater.unimib.it

 © 2006 American Institute of Physics
Downloaded 11 Nov 2009 to 152.78.208.72. Redistribution subject to AIP license or copyright; see http://apl.aip.org/apl/copyright.jsp

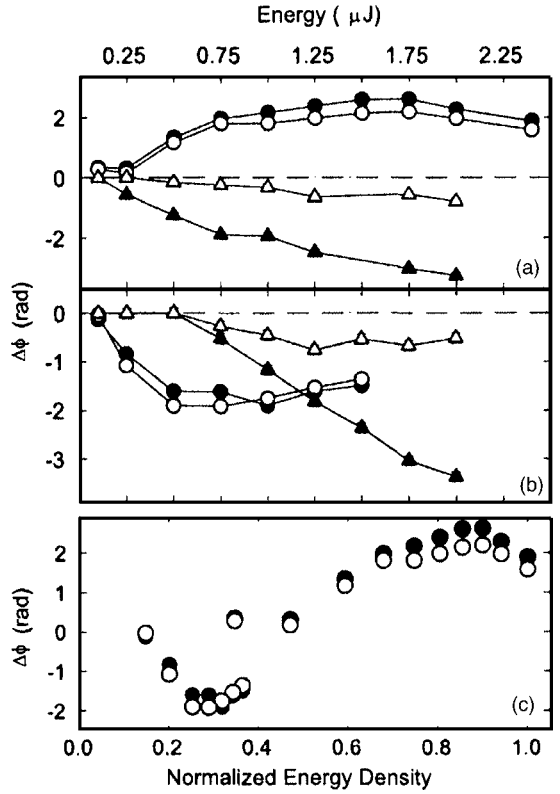

FIG. 2. Phase shift, for polarization parallel (filled marks) and orthogonal (open marks) to the polarization of the writing laser, due to laser-induced refractive index changes in glass (triangles) and SnO_2 containing glass (circles), at (a) high-NA and (b) low-NA focusing of the writing beam vs the laser pulse energy. (c) Phase shift in glassceramics vs the estimated relative value of maximum energy density per pulse along the propagation axis inside the material.

consistent with the negative photosensitivity previously observed with unfocused lasers.[9,10] Remarkably, $\Delta\Phi$ changes sign accordingly to the focusing conditions. No such a change occurs in glass, where negative $\Delta\Phi$ and large birefringence are observed, regardless the NA value, in agreement with previous results.[4,7]

Figure 3(a) shows Raman spectra at different depths from the high-NA irradiated surface of the glass ceramic.

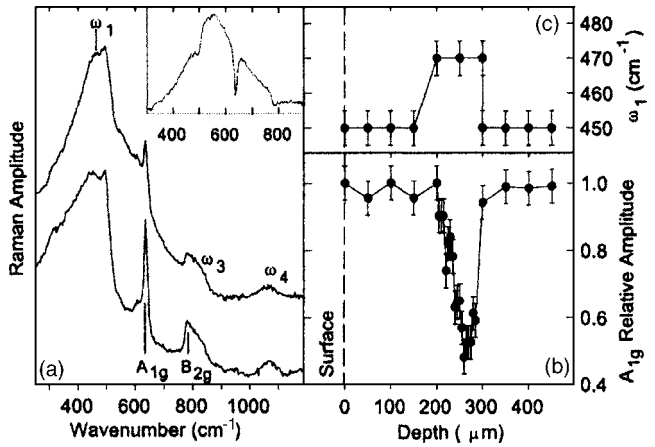

FIG. 3. (a) Confocal micro-Raman spectra at 50 (lower curve) and 250 μm (upper curve) from the sample surface after femtosecond writing at 1.25 μJ of energy pulse. Inset: difference spectrum. (b) Amplitude decrease of the A_{1g} mode of crystalline SnO_2 and (c) energy of the ω_1 silica mode at increasing depth from the front surface of the material.

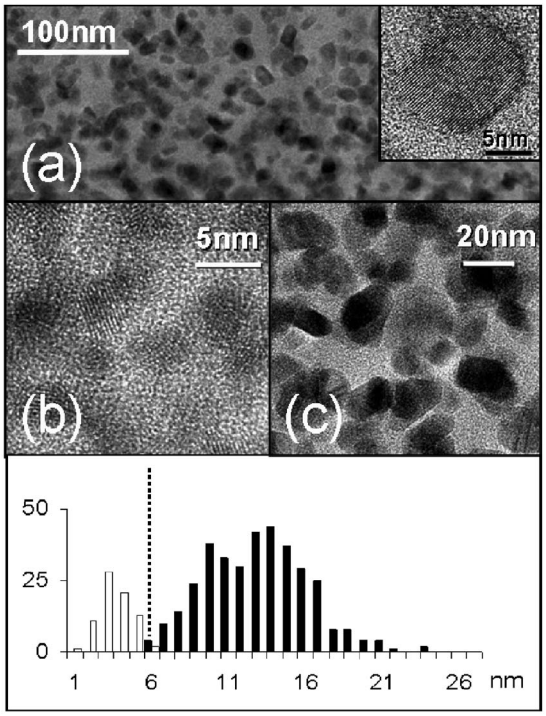

FIG. 4. (a) TEM image of SnO_2 nanoparticles in 16 mol % SnO_2:SiO_2 glass ceramic. Inset: High resolution TEM image of a SnO_2 nanoparticle. (b) Reduced-size and (c) unperturbed-size nanoparticles in laser-processed and -unprocessed regions, respectively, of the material. Histogram: statistics of cluster sizes from sampling of laser-modified (white bars) and -unmodified (black bars) regions.

The A_{1g} mode of SnO_2 (Ref. 11) decreases, approaching the focal plane [Fig. 3(b)], while a broadband grows at 560 cm^{-1} [inset of Fig. 3(a)] ascribable to amorphous SnO_2,[9,11] and the silica ω_1 band[12] shifts at high energy [Fig. 3(c)]. These data indicate a strongly modified buried region of $\approx$50 μm, where the fraction of crystalline nanophase is reduced in favor of an amorphous phase. No detectable change of the A_{1g} mode is observed at low NA. The reference glass does not display any change.

TEM images of the unprocessed material [Fig. 4(a)] show SnO_2 single domain nanocrystals of about 10–15 nm homogeneously dispersed in the glass. However, by sampling the laser-irradiated material, alongside the regions with standard size clusters, micrometer regions containing only nanoclusters smaller than 6 nm are observed [Fig. 4(b)]. Several samplings in the two kinds of regions show distinct size distributions (histogram in Fig. 4).

These results suggest the following comments. The positive phase-shift across the sample written in tighter focusing conditions cannot be interpreted as the superposition of the independent responses of the coexistent phases, both being negative. A model of the interaction between nanophase and silica can be rationalized considering that the decrease of nanocrystal size implies a transformation in an amorphous phase. This kind of transformation should be accompanied by a volume expansion ΔV_{np}. Indeed, the estimated[9] refractive index of laser-induced amorphous SnO_2 (n_a=1.89) is smaller than n_c=1.99 of the crystalline form, consistent with a lower density. The increase of volume of the nanoparticle induces a compression and eventually a compaction in the surrounding silica host, with a positive contribution to Δn. The shift $\Delta\omega_1$ indeed confirms the presence of compressive

Downloaded 11 Nov 2009 to 152.78.208.72. Redistribution subject to AIP license or copyright; see http://apl.aip.org/apl/copyright.jsp

strains into the glass. Nevertheless, we have also to consider that the host resists against the compression and applies in turn a compression to the nanoparticles.

In an attempt to analyze this process, we can quantify the change Δn of refractive index in the modified region from the phase shift $\Delta\Phi$. From the relation $\Delta\Phi = 2\pi\Delta n(d/\lambda) \approx +2$ rad [Fig. 2(a)], taking a thickness $d = 50$ μm [Fig. 3(b)], we obtain approximately $\Delta n = 4\times10^{-3}$. The decrease of the molar fraction y of crystalline SnO_2 in the focal layer with respect to the starting value $y_0 = 0.16$ can in turn be obtained from Raman and TEM analysis. The lowering of the A_{1g} Raman mode suggests a 50% decrease [Fig. 3(b)]. Really, an even higher decrease is expected from a nonperfect rejection of the Raman signal from unperturbed regions. The TEM analysis in fact suggests a 98% reduction of the crystalline phase. In this case, the refractive index change Δn is approximately given by the combination of the changes Δn_{np} and Δn_s in the nanophase and in the surrounding silica, respectively, weighted by the relative phase abundance. The description of the changes Δn_{np} and Δn_s can be treated through the Lorentz-Lorenz (LL) equation[13] $\Delta n = [(n^2-1)(n^2+2)/6n][(\Delta\alpha/\alpha)-(\Delta V/V)]$ for both the silica matrix and the nanophase, where $\Delta V/V$ is the relative volume change, comprising both elastic (compression) and irreversible (compaction) contributions, and $\Delta\alpha/\alpha$ the possible change of ionic polarizability. If we assume that the overall volume of the sample does not change under irradiation, the change of volume of the nanoparticle is compensated by an opposite change of volume of the surrounding silica ($\Delta V_s = -\Delta V_{\mathrm{np}}$). In the LL relation, $\Delta\alpha_{\mathrm{np}}/\alpha_{\mathrm{np}}$ is mainly determined by the structural transformation involved in the nanoparticle amorphization. This process should involve a change of Sn–O coordination, since no sixfold-coordinated amorphous form of oxides is known. $\Delta\alpha_{\mathrm{np}}/\alpha_{\mathrm{np}}$ can be estimated looking at analogous group-IV oxides, SiO_2 and GeO_2, both occurring as fourfold-coordinated glass and sixfold-coordinated crystals. In both cases, $\Delta\alpha/\alpha$ is 11%.[14] If we assume this value and we take[9] $\Delta n_{\mathrm{np}} = -0.1$ as trial value in the LL relation, we finally obtain $\Delta V_{\mathrm{np}}/V_{\mathrm{np}} = 18\%$, corresponding to a silica volume change $\Delta V_s/V_s = -3\%$. Smaller values of $|\Delta n_{\mathrm{np}}|$ and $\Delta V_{\mathrm{np}}/V_{\mathrm{np}}$ are probably more likely, accounting for the host resistance against the nanoparticle expansion. From the experimental Δn and taking $15\% \leqslant (\Delta V_{\mathrm{np}}/V_{\mathrm{np}}) \leqslant 18\%$, we obtain $(\Delta\alpha_s/\alpha_s)/(\Delta V_s/V_s)$ between 0.33 and 0.22, respectively. This ratio is 0.33 for a pure photoelastic response and 0.19 for UV-induced silica compaction.[15] This suggests that the process differs from the UV-induced compaction of silica, specifically for a larger contribution of elastic compression ascribable to the reaction against the nanophase amorphization.

As regards birefringence, in glass ceramics it is smaller than in glass, negligible at low NA. The mechanism occurring in glass, responsible for a form birefringence,[7] is indeed inhibited in glass ceramics because the radiation is prevalently absorbed by nanoparticles, making multiphoton events of glass ionization much more rare.

Finally we consider the origin of the different responses in high- and low-NA configurations. Since the radiation wavelength lies at 800 nm, the observed effects imply two-photon absorption with a ρ^2 dependence on the pulse energy density ρ. An approximate calculation of ρ as a function of the depth z from the surface and the pulse energy E can be carried out accounting for the increase of ρ due to the focused geometry and the decrease due to nonlinear absorption. Within this approximation, the maximum ρ achievable along the z axis is proportional to $[\mathrm{NA}^2E/(1-\mathrm{NA}^2)]^{1/3}$. High-NA and low-NA data, plotted together as a function of this parameter [Fig. 2(c)], indeed disclose a single continuous response behavior.

In summary, SnO_2 nanoparticles trigger a chain of physical mechanisms activated by the interaction with IR femtosecond-laser pulses, providing a flexible tool for the controlled machining of refractive index patterns in silica.

This work was supported by the Italian MIUR.

[1] C. B. Shaffer, J. F. Garcia, and E. Mazur, Appl. Phys. A: Mater. Sci. Process. **76**, 351 (2003).
[2] P. Niay, M. Douay, P. Bernage, W. X. Xie, B. Leconte, D. Ramecourt, E. Delevaque, J. F. Bayon, H. Poignant, and B. Poumellec, Opt. Mater. (Amsterdam, Neth.) **11**, 115 (1999).
[3] J. Canning, K. Sommer, M. Englund, and S. Huntington, Adv. Mater. (Weinheim, Ger.) **13**, 970 (2001).
[4] Y. Shimotsuma, P. G. Kazansky, J. Qiu, and K. Hirao, Phys. Rev. Lett. **91**, 247405 (2003).
[5] K. Miura, J. Qiu, H. Inouye, T. Mitsuyu, and K. Hirao, Appl. Phys. Lett. **71**, 3329 (1997).
[6] J. D. Mills, P. G. Kazansky, E. Bricchi, and J. J. Baumberg, Appl. Phys. Lett. **81**, 196 (2002).
[7] E. Bricchi, B. G. Klappauf, and P. G. Kazansky, Opt. Lett. **11**, 115 (2004).
[8] N. Chiodini, A. Paleari, D. Di Martino, and G. Spinolo, Appl. Phys. Lett. **81**, 1702 (2002).
[9] N. Chiodini, A. Paleari, and G. Spinolo, Phys. Rev. Lett. **90**, 055507 (2003).
[10] N. Chiodini, A. Paleari, G. Spinolo, and P. Crespi, J. Non-Cryst. Solids **322**, 266 (2003).
[11] A. Dieguez, A. Romano-Rodriguez, A. Vila, and J. R. Morante, J. Appl. Phys. **90**, 1550 (2001).
[12] F. L. Galeener, Phys. Rev. B **19**, 4292 (1979).
[13] C. Fiori and R. A. B. Devine, Phys. Rev. B **33**, 2972 (1986).
[14] J. A. Duffy, J. Phys. Chem. B **108**, 14137 (2004).
[15] R. E. Schenker and W. G. Oldham, J. Appl. Phys. **82**, 1065 (1997).

Downloaded 11 Nov 2009 to 152.78.208.72. Redistribution subject to AIP license or copyright; see http://apl.aip.org/apl/copyright.jsp